

See discussions, stats, and author profiles for this publication at: <https://www.researchgate.net/publication/3256544>

AlGa_N/Ga_N/InGa_N/Ga_N DH-HEMTs with an InGa_N notch for enhanced carrier confinement

Article in IEEE Electron Device Letters · February 2006

DOI: 10.1109/LED.2005.861027 · Source: IEEE Xplore

CITATIONS

69

READS

125

5 authors, including:



Yugang Zhou

Nanjing University

26 PUBLICATIONS 792 CITATIONS

[SEE PROFILE](#)



Kei May Lau

The Hong Kong University of Science and Technology

344 PUBLICATIONS 3,986 CITATIONS

[SEE PROFILE](#)



K.J. Chen

The Hong Kong University of Science and Technology

383 PUBLICATIONS 6,114 CITATIONS

[SEE PROFILE](#)

Some of the authors of this publication are also working on these related projects:



Epitaxial Growth of III-V Quantum Dot Lasers on Silicon substrates [View project](#)

AlGaN/GaN/InGaN/GaN DH-HEMTs With an InGaN Notch for Enhanced Carrier Confinement

Jie Liu, *Student Member, IEEE*, Yugang Zhou, Jia Zhu, Kei May Lau, *Fellow, IEEE*, and Kevin J. Chen, *Member, IEEE*

Abstract—We report an AlGaN/GaN/InGaN/GaN double heterojunction high electron mobility transistors (DH-HEMTs) with high-mobility two-dimensional electron gas (2-DEG) and reduced buffer leakage. The device features a 3-nm thin $\text{In}_x\text{Ga}_{1-x}\text{N}$ ($x = 0.1$) layer inserted into the conventional AlGaN/GaN HEMT structure. Assisted by the InGaN layers polarization field that is opposite to that in the AlGaN layer, an additional potential barrier is introduced between the 2-DEG channel and buffer, leading to enhanced carrier confinement and improved buffer isolation. For a sample grown on sapphire substrate with MOCVD-grown GaN buffer, a 2-DEG mobility of around $1300 \text{ cm}^2/\text{V}\cdot\text{s}$ and a sheet resistance of $420 \Omega/\text{sq}$ were obtained on this new DH-HEMT structure at room temperature. A peak transconductance of 230 mS/mm , a peak current gain cutoff frequency (f_T) of 14.5 GHz , and a peak power gain cutoff frequency (f_{max}) of 45.4 GHz were achieved on a $1 \times 100 \mu\text{m}$ device. The off-state source-drain leakage current is as low as $\sim 5 \mu\text{A/mm}$ at $V_{\text{DS}} = 10 \text{ V}$. For the devices on sapphire substrate, maximum power density of 3.4 W/mm and PAE of 41% were obtained at 2 GHz .

Index Terms—Buffer leakage, carrier confinement, double heterojunction (DH), high electron mobility transistors (HEMTs), InGaN.

I. INTRODUCTION

OWING to their high power handling capability at high frequencies, wide bandgap AlGaN/GaN HEMTs are emerging as promising candidates for next-generation RF and microwave power amplifiers. With tremendous progresses made during the last decade in material quality and device processing, AlGaN/GaN HEMTs have been improved significantly in both dc and RF performances [1]–[5]. Meanwhile, more advanced device structures are being explored for further performance improvement. For example, double-channel HEMTs and composite-channel HEMTs have been studied for higher carrier density and improved linearity [6]–[8]. To improve carrier confinement which may result in improved carrier mobility and HEMTs' pinch-off behavior, double-heterojunction HEMTs [9] are also being investigated, following the similar path taken by GaAs PHEMTs and InP HEMTs. Using AlGaN buffer layer with Al composition of 4% [10], Micovic *et al.* demonstrated a GaN double heterojunction HEMT with improved buffer

Manuscript received August 10, 2005; revised October 6, 2005. This work was supported in part by the Hong Kong Research Grants Council and the National Science Foundation of China under Grant N_HKUST616/04, the RGC CERG Grant 61805, and the DAG04/05.EG13. The review of this letter was arranged by Editor T. Mizutani.

The authors are with the Department of Electrical and Electronic Engineering, Hong Kong University of Science and Technology, Kowloon, Hong Kong (e-mail: liujie@ust.hk; eekjchen@ust.hk).

Digital Object Identifier 10.1109/LED.2005.861027

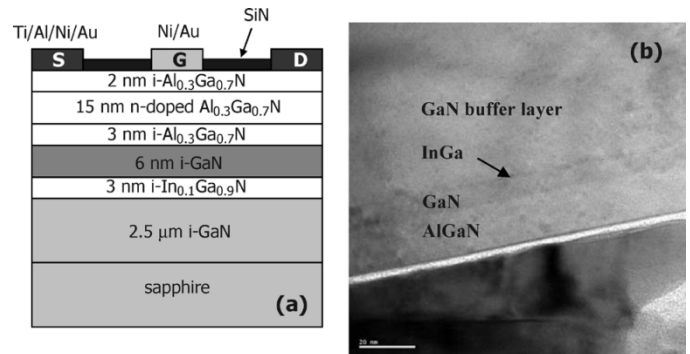


Fig. 1. (a) Schematic cross section of the AlGaN/GaN/InGaN/GaN DH-HEMT and (b) TEM cross section picture, with a well-defined GaN/InGaN interface.

isolation. However, a high Al composition in the AlGaN buffer layer is still difficult to achieve. Simin *et al.* has implemented AlGaN/InGaN/GaN HEMTs and MOSHFETs [11], [12] in which InGaN has been used as the channel material which is confined from both sides by AlGaN and GaN. However, it is challenging to grow cluster-free high-mobility InGaN layer. The highest 2-DEG mobility reported in the AlGaN/InGaN/GaN DH-HEMTs is $730 \text{ cm}^2/\text{V} \cdot \text{s}$ [11], [12], significantly lower than that achieved in conventional AlGaN/GaN HEMTs. In this letter, we report an AlGaN/GaN/InGaN/GaN DH-HEMT that features an InGaN-notch in the channel region. Since the GaN layer remains as the major channel, the mobility degradation that usually occurs in InGaN layer is avoided. On the other hand, owing to the opposite piezoelectric polarization field in the InGaN layer [13], [14], an additional potential barrier is created between the channel and the buffer layer. This additional barrier leads to better carrier confinement and better buffer isolation, which in turn, enables improved device performance, i.e., higher 2-DEG mobility and lower leakage current.

II. DEVICE STRUCTURE AND FABRICATION

The AlGaN/GaN/InGaN/GaN DH-HEMT structure, with the schematic cross section shown in Fig. 1(a), was grown on (0001) sapphire substrates in an Aixtron AIX 2000 HT MOCVD system. After initial desorption at $1200 \text{ }^\circ\text{C}$, a GaN nucleation layer was grown at $550 \text{ }^\circ\text{C}$, followed by a $2.5\text{-}\mu\text{m}$ -thick unintentionally doped GaN buffer layer. Then the InGaN-notch layer, which is 3 nm thick with 10% indium composition, was grown with pure nitrogen carrier gas at $810 \text{ }^\circ\text{C}$. Ammonia (NH_3), trimethyl-gallium (TMG) and trimethyl-indium (TMI) were used as source materials. It is followed by the 6-nm -thick GaN channel layer grown at $810 \text{ }^\circ\text{C}$. The barrier layer was grown at $1100 \text{ }^\circ\text{C}$, which consists of a 3-nm undoped spacer, a 15-nm

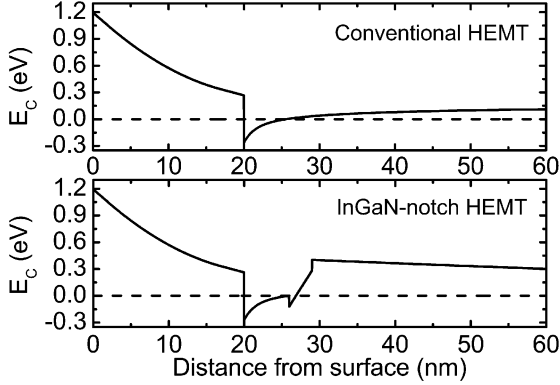


Fig. 2. Calculated conduction band diagram of the (top) conventional HEMT and (bottom) the DH-HEMT.

doped ($2 \times 10^{18} \text{ cm}^{-3}$) carrier supplier layer doped at, and a 2-nm undoped cap layer. The carrier gas used for the GaN and AlGaN layers is hydrogen. Fig. 1(b) shows the cross-sectional transmission electron microscopy (TEM) picture of the sample. A well-defined InGaN layer was observed at about 6 nm from the AlGaN/GaN hetero-interface, which indicates that a good quality InGaN layer was successfully grown. The carrier gas used in the growth of GaN and AlGaN is hydrogen. Device active regions were defined using mesa etching by inductively coupled plasma reactive ion etching (ICP-RIE). It is followed by the source/drain ohmic contacts formation by a rapid thermal annealing of e-beam evaporated Ti/Al/Ni/Au at $850 \text{ }^\circ\text{C}$ for 30 s. Using on-wafer transfer length method (TLM) patterns, the ohmic contact resistance was typically measured to be $0.8 \text{ } \Omega\cdot\text{mm}$. Gate electrodes with $1 \text{ } \mu\text{m}$ length were then defined by contact photolithography, Ni/Au e-beam evaporation and lift-off, subsequently. The devices have a source-gate spacing of $L_{\text{sg}} = 1 \text{ } \mu\text{m}$ and a gate-drain spacing of $L_{\text{gd}} = 1 \text{ } \mu\text{m}$. Finally, the devices were passivated using PECVD-grown SiN.

III. DEVICE CHARACTERISTICS AND DISCUSSION

The conduction band profile of the AlGaN/GaN/InGaN/GaN DH-HEMT is calculated by solving the Poisson's equation and is plotted in Fig. 2, along with that of a conventional AlGaN/GaN HEMT. The conduction-band offset at InGaN/GaN hetero-interface and the polarization charge density in the InGaN layer are set to be $\Delta E_C = 0.12 \text{ eV}$ and $6.68 \times 10^{12} \text{ e/cm}^2$, respectively [13]. Due to the opposite piezoelectric polarization in the InGaN layer compared to the AlGaN layer, the conduction band at the hetero-interface between the InGaN-notch and GaN buffer is raised and a sharp potential barrier is formed at the back of 2-DEG channel. Such a barrier can help confine the electrons better and reduce the electron spillover to the buffer layer. As shown in Fig. 2, the conduction band at the GaN/InGaN interface falls below the Fermi level and a minor channel can be formed. However, electrons in this minor channel are not confined well and can easily spill over to the major channel. No distinctive device characteristics are expected from this minor channel. Extensive simulation was carried out to reach the final design of the epi-structure. The InGaN layer was designed to be as thin as 3 nm to achieve two goals: 1) obtain a potential barrier larger

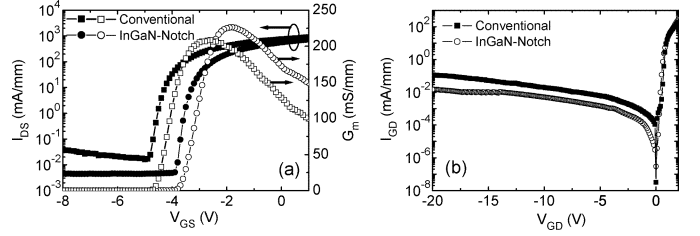


Fig. 3. DC characteristics of DH-HEMT (circle) and conventional HEMT (square): (a) The transfer and transconduction characteristics at $V_{\text{DS}} = 10 \text{ V}$; (b) the I - V characteristics of the gate-drain Schottky diode.

than 300 meV at the back of the channel and 2) layer thickness is kept as thin as possible to reduce the risk of indium cluster formation. Based on cross-sectional TEM, no indium clusters were observed.

Room-temperature Hall measurements of the DH-HEMT structure was performed on a Hall bridge pattern fabricated on wafer by photolithography, which yielded an electron mobility of $1300 \text{ cm}^2/\text{V}\cdot\text{s}$ and a sheet resistance of $420 \text{ } \Omega/\text{sq}$. Unlike some other works [11], [12], the mobility obtained in this letter is higher than that of our conventional AlGaN/GaN HEMT devices, which is normally around $1000 \text{ cm}^2/\text{V}\cdot\text{s}$, with a sheet resistance of $440 \text{ } \Omega/\text{sq}$. This indicates that the inserted InGaN-notch layer plays positive role in enhancing the 2-DEG confinement and then improving the mobility. The sheet carrier density in the InGaN-notch HEMTs is $9.84 \times 10^{12} \text{ cm}^{-2}$, which is lower than the value in our conventional HEMTs ($1.38 \times 10^{13} \text{ cm}^{-2}$). The lower carrier density is due to GaN channels potential being pulled up by the InGaN notch. Such a potential rise is also reflected in the devices threshold voltage, which shifts positively, as shown later in this letter.

The transfer characteristics of the DH-HEMT, in comparison with those of the conventional AlGaN/GaN HEMTs, are plotted in Fig. 3(a). The maximum drain current density of the DH-HEMT is 850 mA/mm in a $1 \times 10 \text{ } \mu\text{m}$ device. The pinch-off voltage of the DH-HEMT is about -4 V , with an off-state breakdown voltage larger than 60 V . The positive shift of the pinch-off voltage in the DH-HEMT is due to the polarization field in the InGaN layer, which is opposite to that in the AlGaN barrier. A peak transconductance of about 230 mS/mm is obtained in the DH-HEMT, which is about 10% higher than that achieved in our conventional HEMT devices. The buffer leakage current density of a $1 \times 10 \text{ } \mu\text{m}$ DH-HEMT device is about $5 \text{ } \mu\text{A/mm}$ at $V_{\text{DS}} = 10 \text{ V}$, significantly lower than that in our conventional HEMT devices ($\sim 20 \text{ } \mu\text{A/mm}$). The reduced leakage current strongly indicates that the potential barrier between the channel and the buffer layer can effectively improve the buffer isolation. The I - V characteristics of the gate-drain Schottky diode of the DH-HEMT and conventional HEMT are shown in Fig. 3(b), the DH-HEMT also shows a lower gate leakage current than the conventional one.

On-wafer S -parameters measurement was conducted on a $1 \times 100 \text{ } \mu\text{m}$ DH-HEMT device. The gate-bias-dependent current gain and power gain cutoff frequencies, f_T and f_{max} , were extracted and plotted in Fig. 4 together with the results of the conventional HEMT. A maximum f_T of 14.5 GHz and a f_{max} of 45.4 GHz were obtained in the DH-HEMT devices. The peak

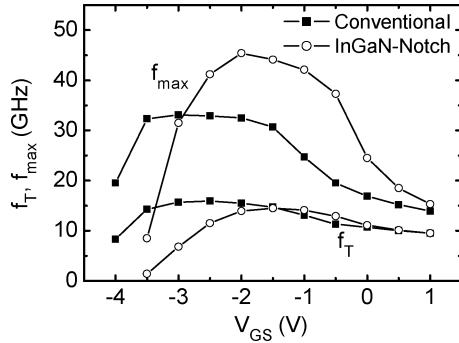


Fig. 4. Extracted current gain and power gain cutoff frequencies f_T , f_{max} of the conventional and DH-HEMTs. V_{DS} is biased at 10 V.

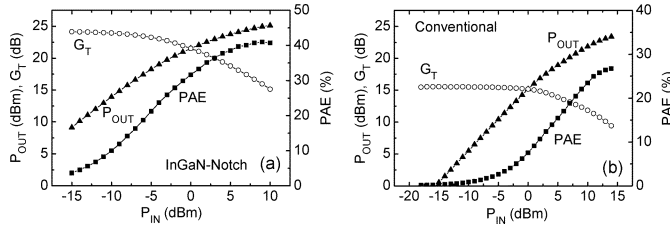


Fig. 5. Large-signal load-pull characterization at 2 GHz of the (a) DH-HEMT and (b) conventional HEMT. The quiescent bias point is $V_{DS} = 35$ V, $I_{DS} = 15\% I_{max}$.

value of f_T on the InGaN-notch HEMT is slightly lower than that in the conventional one. Significant improvement, as large as 37%, can be observed in the peak f_{max} . This is attributed to the reduction in the buffer leakage current that results in larger output source-drain resistance, R_{DS} . In the first order approximation, f_{max} is related to f_T in the following equation [15], $(f_{max}/f_T) = (1/2)(R_{DS}/R_G + R_{CH})^{1/2}$. R_G is the gate resistance; and R_{CH} is the channel charging resistance. As R_{DS} increases in the InGaN-notch HEMT, f_{max} is also increased.

Large-signal load-pull measurement was carried out using Maurys MT982B01 tuners. Tuning for maximum output power (P_{out}) at 2 GHz, a P_{out} of 3.4 W/mm (and 2.2 W/mm) and a peak PAE of 41% (27%) were obtained with a 35 V drain supply voltage, in the InGaN-notch (and conventional) HEMTs, as shown in Fig. 5.

IV. CONCLUSION

A novel AlGaIn/GaN/InGaIn/GaN DH-HEMT with improved 2-DEG mobility has been demonstrated on sapphire substrate. The inserted InGaIn-notch layer plays a key role in reducing buffer leakage and improving 2-DEG mobility. The InGaIn layer has an opposite piezoelectric polarization field compared to AlGaIn, which results in a very sharp rise of the conduction band below the 2-DEG channel. The raised potential barrier for

the electrons can help enhance the confinement of the 2-DEG, and then improve the electron mobility. The potential barrier also prevents 2-DEG from spilling over to the buffer layer, and therefore, assists in reducing the buffer leakage current. The electron mobility obtained this DH-HEMT structure is shown to be 30% higher than that obtained in a conventional AlGaIn/GaN single heterojunction HEMT structure.

REFERENCES

- [1] U. K. Mishra, P. Parikh, and Y. F. Wu, "AlGaIn/GaN HEMTs—an overview of device operation and applications," *Proc. IEEE*, vol. 90, no. 6, pp. 1022–1031, Jun. 2002.
- [2] K. Joshin, T. Kikkawa, H. Hayashi, S. Yokogawa, M. Yokoyama, N. Adachi, and M. Takikawa, "A 174 W high-efficiency GaN HEMT power amplifier for W-CDMA base station applications," in *IEDM Tech. Dig.*, Dec. 2003, pp. 983–985.
- [3] Y. F. Wu, A. Saxler, M. Moore, R. P. Smith, S. Sheppard, P. M. Chavarkar, T. Wisleder, U. K. Mishra, and P. Parikh, "30-W/mm GaN HEMTs by field plate optimization," *IEEE Electron Device Lett.*, vol. 25, no. 3, pp. 117–119, Mar. 2004.
- [4] M. Kanamura, T. Kikkawa, and K. Joshin, "A 100-W high-gain AlGaIn/GaN HEMT power amplifier on a conductive N-SiC substrate for wireless base station applications," in *2004 IEDM Tech. Dig.*, San Francisco, Dec. 13–15, 2004, pp. 799–802.
- [5] Y. F. Wu, M. Moore, T. Wisleder, P. M. Chavarkar, U. K. Mishra, and P. Parikh, "High-gain microwave GaN HEMTs with source-terminated field-plates," in *IEDM Tech. Dig.*, San Francisco, Dec. 13–15, 2004, pp. 1078–1079.
- [6] R. M. Chu, Y. G. Zhou, J. Liu, D. Wang, K. J. Chen, and K. M. Lau, "AlGaIn-GaN double-channel HEMTs," *IEEE Trans. Electron Devices*, vol. 52, no. 4, pp. 438–446, Apr. 2005.
- [7] J. Liu, Y. G. Zhou, R. M. Chu, Y. Cai, K. J. Chen, and K. M. Lau, " $Al_{0.3}Ga_{0.7}N/Al_{0.05}Ga_{0.95}N/GaN$ composite-channel HEMTs with enhanced linearity," in *IEDM Tech. Dig.*, San Francisco, Dec. 13–15, 2004, pp. 811–814.
- [8] —, "Highly linear $Al_{0.3}Ga_{0.7}N/Al_{0.05}Ga_{0.95}N/GaN$ composite-channel HEMTs," *IEEE Electron Device Lett.*, vol. 26, no. 3, pp. 145–147, Mar. 2005.
- [9] N. Maeda, T. Saitoh, K. Tsubaki, T. Nishida, and N. Kobayashi, "Enhanced effect of polarization on electron transport properties in AlGaIn/GaN double-heterostructure field-effect transistors," *Appl. Phys. Lett.*, vol. 76, no. 21, pp. 3118–3120, May 2000.
- [10] M. Micovic *et al.*, "GaN double heterojunction field effect transistor for microwave and millimeterwave power applications," in *IEDM Tech. Dig.*, San Francisco, Dec. 13–15, 2004, pp. 807–810.
- [11] G. Simin, X. Hu, A. Tarakji, J. Zhang, A. Koudymov, S. Saygi, J. Yang, M. A. Khan, M. Shur, and R. Gaska, "AlGaIn/InGaIn/GaN double heterostructure field-effect transistor," *Jpn. J. Appl. Phys.*, vol. 40, no. 11A, pp. L1142–L1144, Nov. 2001.
- [12] G. Simin, A. Koudymov, H. Fatima, J. Zhang, J. Yang, M. A. Khan, X. Hu, A. Tarakji, R. Gaska, and M. Shur, " $SiO_2/AlGaIn/InGaIn/GaN$ MOSDFETs," *IEEE Electron Device Lett.*, vol. 23, no. 8, pp. 458–460, Aug. 2002.
- [13] O. Ambacher *et al.*, "Pyroelectric properties of Al(In)GaIn/GaN hetero- and quantum well structures," *J. Phys. Condens. Matter*, vol. 14, pp. 3399–3434, 2002.
- [14] H. Zhang, E. J. Miller, E. T. Yu, C. Poblenz, and J. S. Speck, "Measurement of polarization charge and conduction-band offset at $In_xGa_{1-x}N$ heterojunction interfaces," *Appl. Phys. Lett.*, vol. 84, no. 23, pp. 4644–4646, Jun. 2004.
- [15] J. M. Golio, *Microwave MESTETs & HEMTs*. Boston, MA: Artech House, 1991, p. 299.